Sensors and Actuators B 157 (2011) 216–224

Contents lists available at ScienceDirect

Sensors and Actuators B: Chemical

journal homepage: www.elsevier.com/locate/snb

Targeting of multiple metabolites in neural cells monitored by using protein-based carbon nanotubes

Cristina Boero[a,*], Sandro Carrara[a], Giovanna Del Vecchio[b], Laura Calzà[b], Giovanni De Micheli[a]

[a] Laboratory of Integrated Systems, EPFL, Lausanne 1015, Switzerland
[b] DIMORFIPA, University of Bologna, Ozzano dell'Emilia (BO) 40126, Italy

ARTICLE INFO

Article history:
Received 4 February 2011
Received in revised form 21 March 2011
Accepted 24 March 2011
Available online 31 March 2011

Keywords:
Electrochemical biosensor
Metabolite
Cell culture
Carbon nanotubes
Oxidase
Glucose deprivation

ABSTRACT

Microdevices dedicated to monitor metabolite levels have recently enabled many applications in the field of cell analysis, to monitor cell growth and development of numerous cell lines. By combining the traditional technology used for electrochemical biosensors with nanoscale materials, it is possible to develop miniaturized metabolite biosensors with unique properties of sensitivity and detection limit. In particular, enzymes tend to adsorb onto carbon nanotubes and their optical or electrical activity can perturb the electronic properties. In the present work we propose multi-walled carbon nanotube-based biosensors to monitor a cell line highly sensitive to metabolic alterations, in order to evaluate lactate production and glucose uptake during different cell states. We achieve sensors for both lactate and glucose, with sensitivities of 40.1 $\mu A\,mM^{-1}\,cm^{-2}$ and 27.7 $\mu A\,mM^{-1}\,cm^{-2}$, and detection limits of 28 μM and 73 μM, respectively. This nano-biosensing technology is used to provide new information on cell line metabolism during proliferation and differentiation, which are unprecedented in cell biology.

1. Introduction

Metabolite monitoring in cell cultures is of crucial importance for a wide range of applications: it is a further instrument to deep understand cell mechanisms; it can help to develop automated systems for tissue engineering; it can be applied to investigate gene-expression pathways in cell biology. Important biological metabolites are sometime difficult to measure *in vitro* or in real-time. Standard techniques such as immunoassays, gel electrophoresis and nuclear magnetic resonance typically cannot be performed in live cells and tissues, or at least they require preparation steps that inhibit real-time measurements [1]. Instead, electrochemical sensing based on oxidases is suitable for real-time monitoring of metabolites, such as glucose [2] and lactate [3].

In the field of electrochemical techniques for compound detection, sensing by using nanoscale materials offers a unique opportunity to improve sensitivity while protein probes improve specificity. It is well known that carbon nanotubes (CNT) have considerable electron field emission properties. They are used to enhance the emissivity of electrodes made of various materials [4]. Many theoretical [5,6] and experimental [7] works have been published related to CNT field. The results suggest that the major contribution to emission performance is mainly from the body (the sidewall) of each individual CNT. From the biosensing point-of-view, increased emission performance from CNT definitely results in an improved sensitivity of sensors for metabolites [8]. Moreover, molecular adsorption of proteins onto carbon nanotubes can be translated into an optical [9] or electrical [10] signal by perturbing the electronic structure of the nanotubes. Thus, their functionalization with enzymes offers a unique way to improve also the specificity of the detection.

Among all the metabolites which can be monitored, certainly glucose is the most interesting, since it is the essential source of energy for the body, and especially for the brain. Although glucose is traditionally considered as the preferential source of energy for neurons, recent papers suggest that lactate might be transported within the different brain cell types (e.g. neurons and astrocytes), and consumed instead of glucose during neuronal activation [11]. Therefore, the so-called astrocyte-neuron shuttle model proposes a net production of glutamate-derived lactate by astrocytes, which is then transported and consumed by neurons [12]. However, no definitive data are available to support this theory, making this field of research very debated [13].

To this purpose, the use of sensor arrays combining carbon nanotubes and enzymes for sensing levels of such metabolites can definitely contribute to elucidate this point. One of the simplified biological systems, e.g. neuronal cultures in dynamic metabolic conditions is the SN56 cell line, which derives from fusion of septal neurons of postnatal mice with murine neuroblastoma cells. SN56 is a cholinergic line, and cholinergic neurons are highly sen-

* Corresponding author. Tel.: +41 21 693687; fax: +41 21 6930909.
E-mail address: cristina.boero@epfl.ch (C. Boero).

0925-4005/$ – see front matter © 2011 Elsevier B.V. All rights reserved.
doi:10.1016/j.snb.2011.03.053

sitive to several stressors and to metabolic alterations. Those cells actively proliferate, but they acquire mature cholinergic phenotype after retinoic acid (RA) exposure, which also stops cell cycle. Therefore, depending on RA administration, we will refer to proliferation state of neuron precursors in the case we do not supply the acid; otherwise cells differentiate in mature neurons, similarly to the case of stem cells. Thus, on one side SN56 represents a suitable model to test the hypothesis astrocyte-neuron shuttle model [12]; on the other side they "mimic" stem cell behavior, allowing the investigation of cell metabolism during different cell states.

In the present work we develop biosensors nanostructured with multi-walled carbon nanotubes (MWCNT) and we exploit them for sensing relevant metabolites in SN56 cell line. We show how proteins arrange themselves onto carbon nanotube surface. We calibrate the biosensors for the detection of glucose and lactate in cell medium. We monitor glucose uptake and lactate production during proliferative and differentiate states. Finally, we investigate lactate concentration in conditions of glucose deprivation, showing direct confirmation of the hypothesis on metabolite transportation. Thus, we demonstrate that the proposed method is suitable for stem cell monitoring as well as cell biology investigations.

2. Material and methods

2.1. Reagents

Carbon paste Screen-printed electrodes (SPE - model DRP-110) and multi-walled carbon nanotubes were purchased from Dropsens (Spain). Carbon nanotubes (diameter 10 nm, length 1–2 μm) were purchased in powder (90% purity), and subsequently diluted in chloroform to the concentration of 1 mg ml^{-1} [8]. Samples were then sonicated in order to obtain a homogeneous solution. Glucose oxidase from *Aspergillus Niger* (GOD, EC 1.1.3.4, 129.9 units/mg solid), lactate oxidase from *Pediococcus* species (LOD, EC 1.13.12.4, ≥20 units/mg solid), D-(+)-glucose, and lithium L-lactate were purchased from Sigma–Aldrich (Switzerland) in lyophilized powder. All the proteins were dissolved in Phosphate Buffer Saline (PBS) 0.01 M at pH 7.4, while glucose and lactate were dissolved in Milli-Q.

2.2. Apparatus

The electrochemical response of the functionalized MWCNT for glucose or lactate detection is investigated by chronoamperometry under aerobic conditions. Electrochemical measurements are acquired by using Versastat 3 potentiostat (Princeton Applied Technologies). Experiments are carried out using a conventional three-electrode system. The screen-printed electrode consists of a graphite working electrode, which presents an active area equal to 13 mm^2; a counter electrode, also made of graphite; a reference electrode, made of Ag/AgCl. The total area of the cell is 22 mm^2.

Imaging of multi-walled carbon nanotubes are acquired by using a Philips/FEI XL-30 F (Netherlands) scanning electron microscope (SEM). The resolution in UHR mode is 2.5 nm at 1 kV. Pictures of living cells are captured by inverted Olympus IX70 optical microscope equipped with a digital photo camera Camedia C-5060 and phase 100 contrast filter. Fluorescent images are captured with a Nikon Eclipse E600 microscope equipped 101 with a Nikon Digital Camera DXM1200 (ATI system) appropriate filters for fluorescence staining.

2.3. Nanostructured electrodes preparation

To prepare nanostructured electrodes, 40 μl of MWCNT-chloroform solution is spread (in drops of 5 μl each) onto the working electrode and allowed to dry.Then, the MWCNT are functionalized by using the probe enzyme in order to obtain biosensors for glucose and lactate detection. A volume of 20 μl of glucose or lactate oxidase (15 mg ml^{-1} and 125 mg ml^{-1}, respectively) is dropped onto the MWCNT and stored overnight at +4 °C, in order to allow protein adsorption onto the electrode surface. Then, the drop is rinsed out with Milli-Q and the electrode is conditioned for 10 min at constant potential (+550 mV) before the first use. All the functionalized electrodes are stored at +4 °C and covered with PBS, after use.

2.4. Cell culture

SN56 cell line (clone SN56.B5.G4), derived from the fusion of septal neurons of postnatal day 21 mice with N18TG2 murine neuroblastoma cells [14], is a generous gift of Prof. Bruce H. Wainer (Emory University, Atlanta, GA, USA). Proliferating cells are maintained in Dulbecco's modified Eagle's medium (DMEM, Sigma, Saint Louis, Missouri USA), supplemented with 10% Foetal Bovine Serum (FBS, Gibco/BRL, Rockville, MD, USA), 2 mM L-glutamine (Sigma), and 40 U/ml penicillin/streptomycin (Gibco), in 25 cm^2 culture flasks (Corning, New York, NY USA) in a 5% CO_2 atmosphere at 37 °C. Medium in the stock flasks is changed every 48 h and the cells are sub-cultured when they reached 80–90% of confluence. Cells are seeded at 5×10^3, 2.5×10^4, 2×10^5 cell cm^{-2}, after four passages from thawing. Then, cells are cultured onto uncoated wells in proliferating conditions for 48 h or onto poly-L-lysine (Sigma)-coated wells when induced to differentiate, with or without covers lips, depending on the experiment. Differentiating cells are let adhere to coated substrates for further 48 h in the same, but serum free, growth medium; afterwards, they are supplemented with 1 μM all-trans-retinoic acid (RA) from Sigma–Aldrich (Switzerland) for 48 h [15]. Surnatant conditioned medium is collected for glucose and lactate level measurements at 4, 24 and 48 h after RA supply.

2.5. Glucose deprivation

After 48 h of proliferation and induction of differentiation by RA treatment, cells at 2.5×10^4 are subjected to glucose deprivation. Briefly, complete medium (glucose 22.4 mM) is removed and cells are washed twice with glucose-free DMEM (Cat N° D5030, Sigma, Switzerland), 2 mM L-glutamine (Sigma), 44 mM $NaHCO_3$ (Sigma), 40 U/ml penicillin/streptomycin, supplemented or not with FBS. Cells are glucose-deprived for 48 h by using the glucose-free medium described above.

2.6. MTT assay

Cell growth and viability are studied by MTT biochemical approach on cells seeded at 2.5×10^4, based on the reduction of MTT (3-[4,5-dimethylthiazol-2-yl]-2,5-diphenyl tetrazolium bromide, Sigma) into formazan crystals by the action of the mitochondrial dehydrogenase enzymes present in viable cells. The so-formed crystals are then dissolved in acidified isopropanol, giving a spectrophotometrically measurable purple solution. Cells are treated with a solution of 5 mg ml^{-1} of MTT. After 2 h at 37 °C the formed formazan crystals are dissolved in a solution consisting of 10% Triton X-100/0.1 N HCl/isopropanol and incubated for 1 h at room temperature in the dark. Absorbance is read at a wavelength of 570 nm. Blanks are prepared as the same way as samples but without cells. Absorbance values correspond to the number of viable cells.

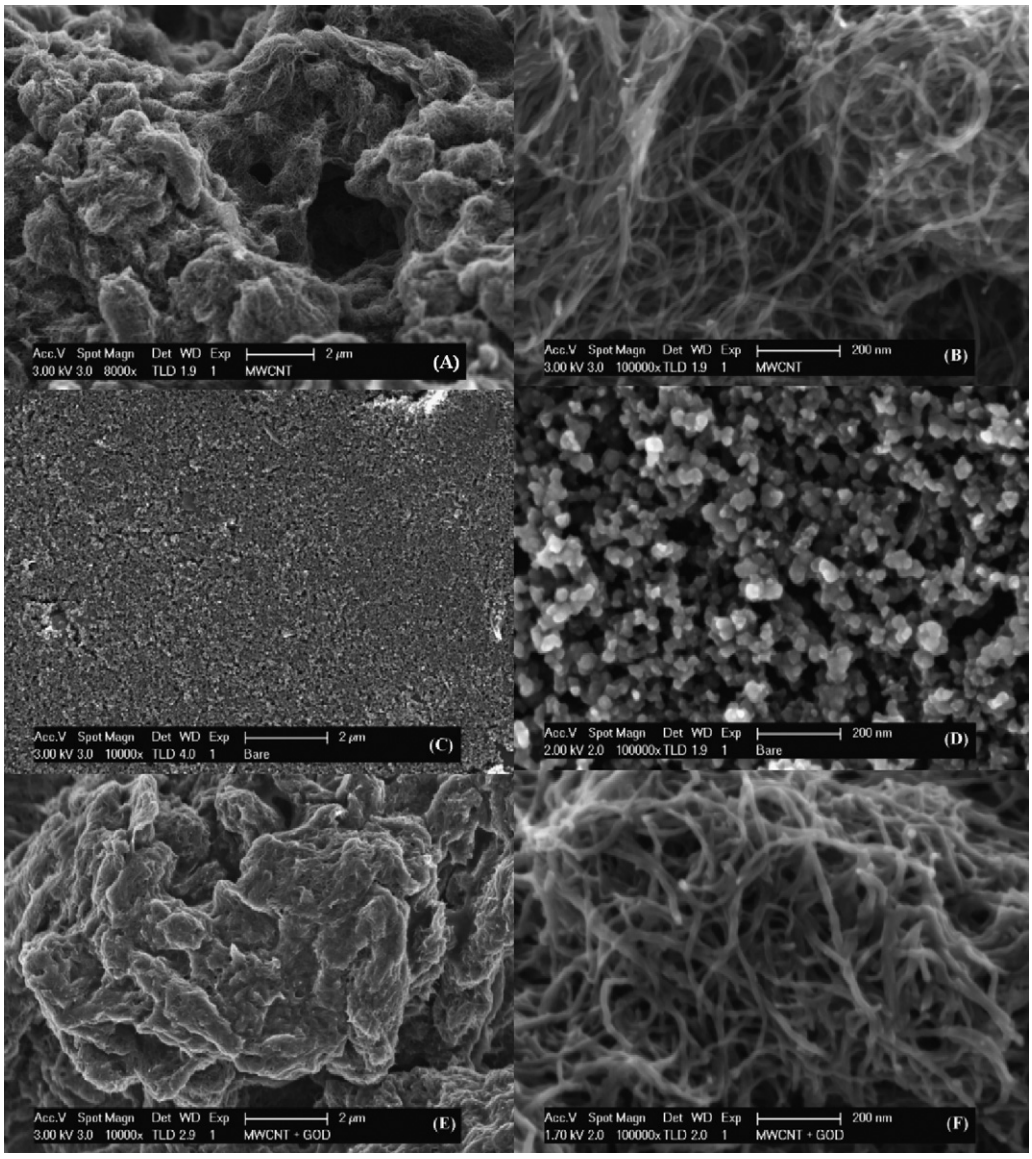

Fig. 1. SEM images of multi-walled carbon nanotubes. (A) and (B) illustrate MWCNT drop-cast onto screen-printed electrodes from a chloroform solution of mono-dispersed tubes; (C) and (D) depict the surface of the screen-printed electrodes without MWCNT; E and F show MWCNT functionalized by using glucose oxidase. Images acquired in the case of MWCNT functionalized by using lactate oxidase are similar to pictures (E) and (F) (data not shown).

2.7. Immunocytochemistry

Cells are seeded at a density of 2.5×10^4 cells cm^{-2}. At the appropriate time points, cells are washed with ice-cold phosphate buffered saline and fixed with a solution of 4% ice-cold para-formaldehyde for 20 min at 4 °C followed by PBS washes. The following antisera have been used in this study: intracellular $p75_{NTR}$ 1:600 (Rabbit, anti-p75, Promega Corporation, Madison, WI, USA), 1:200, ChAT (Goat, anti-ChAT, Chemicon International, Temecula, CA, USA) 1:500; BetaIII-Tubulin at 1:1000 (Mouse, anti-BetaIII Tubulin, R&D, R&D systems, Minneapolis, MN, USA). Cells are then incubated for 30 min at 37 °C with secondary antibodies (Donkey anti-goat and anti-mouse cy-2, at 1:100; donkey anti-rabbit RRX at 1:100) (all from Jackson Immunoresearch laboratories, West Grove, PA, USA). After immunofluorescence staining, cells are incubated with the nuclear dye Hoechst33258 (1 μg ml^{-1} in PBS, 0.2% TritonX-100) for 20 min at room temperature, washed with PBS and mounted in a solution containing para-phenylendiamine to reduce fading.

3. Results and discussion

3.1. Enzyme immobilization

Fig. 1 shows acquired SEM pictures of carbon nanotubes cast onto screen-printed electrodes, and functionalized with oxidases. Since nanotubes walls are highly hydrophobic [16], they tend to form bundles, as depicted in Fig. 1A, even if they consist of individual carbon fibers, as detailed in Fig. 1B. The morphology of nanostructured electrodes is clearly related to carbon nanotubes (CNT) properties, as demonstrated by the flatness of the bare electrode surface (Fig. 1C), where graphite nanoparticles can be clearly identified (Fig. 1D). In the case of nanotubes functionalized with enzymes, the protein layer entirely covers the free-space within bundles (Fig. 1E), and wraps each carbon nanotube (Fig. 1F). The fiber size spans from 10.98 ± 1.64 nm, in the case of CNT, up to 18.90 ± 2.09 nm, in the case of CNT functionalized with glucose oxidase. The glucose oxidase (GOD) from *Aspergillus niger* is illustrated in Fig. 2A and B, which structure has been obtained at 1.9 Å reso-

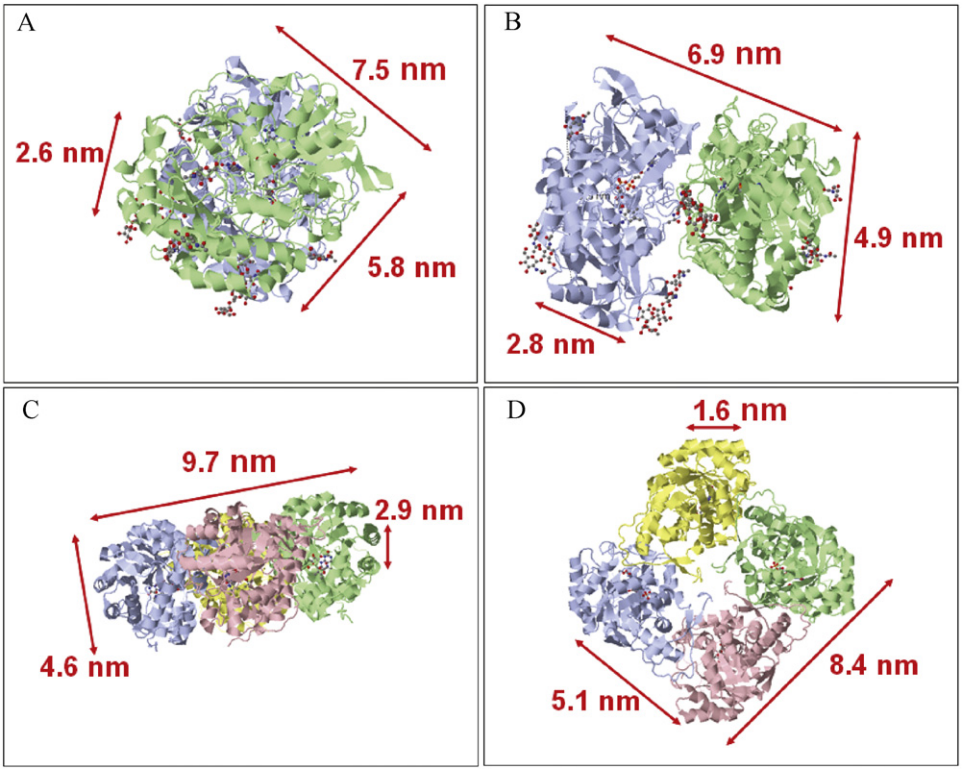

Fig. 2. Crystallographic 3D structure of oxidases. Lateral (A) and top (B) view of glucose oxidase from *penicillium amagasakiense* are depicted in the on the top of the figure. Lateral (C) and top (D) view of lactate oxidase with pryruvte complex are illustrated on the bottom. Both images have a resolution of 1.9 Å. Glucose oxidase is a two sub-units protein, which may be included within a cube with size equal to 10 nm × 9 nm × 8 nm, while lactate oxidase is a protein with 4 sub-units approximately sized 4.6 nm × 5 nm × 4 nm. The whole protein structure can be included within a cube with size equal to 9 nm × 8 nm × 5 nm. The two protein structures are from RCSB Protein Databank (http://www.rcsb.org)

lution [17]. It is composed by two sub-units with individual size ranging from 3 up to 7.5 nm. Similarly, the lactate oxidase is a protein composed by four sub-units, which measure within 4.6 and 9.7 nm, as shown in Fig. 2C and D. Lactate oxidase (LOD) from *Aerococcus viridans* has been investigate in interaction with pyruvate and the LOD-pyruvate complex has been solved at a resolution of 1.90 Å resolution [18]. Crystallographic models confirm that size enlargement measured in SEM images is compatible with a single layer of proteins around the nanotubes.

3.2. Biosensor calibration

For calibration and investigation of the detection limit, the electrode is dipped into the PBS solution with a volume of 25 ml under stirring conditions. A volume of 25 μl per step of the target molecule is successively added into the solution with a time-step of 2 min. To perform measurements, we apply a potential of +550 mV vs. Ag/AgCl, which corresponds to the oxidation potential of hydrogen peroxide [19]. For glucose biosensor, we obtain a sensitivity of 27.7 $\mu A\,mM^{-1}\,cm^{-2}$, a linear range within 0.5–4.0 mM, and detection limit of 73 μM (considering a signal-to-noise ratio of 3). For lactate detection, we achieve a sensitivity of 40.1 $\mu A\,mM^{-1}\,cm^{-2}$, a linear range within 0.5–2.5 mM, and detection limit of 28 μM (data not shown).

For medium measurements, we change a little bit the experimental setup. Instead of dipping the sensor into the solution, since we work with small cell flasks, we perform measurements in quiescent conditions. For this reason, for each new electrode we perform a two-point calibration with nominal concentration in diluted DMEM, before measuring medium coming from the cell culture. Hence, screen-printed electrodes are covered with a drop of 100 μl of diluted medium. For glucose calibration the DMEM is used as it is, while lactate is added for the calibration in the case of lactate sensor calibration. The rate of dilution is chosen according to the fact that the concentration of glucose in DMEM used for the present experiments is of 22.4 mM ($4.5\,g\,l^{-1}$). Since it is not possible to perform measurements in pure DMEM, due to the interferences arising from easily electro-oxidizable compounds at the same oxidation potential, all the measurements are performed in 1:10 diluted DMEM in PBS, so that the maximum concentration of interest is 2.24 mM. From the calibration curves it is possible to notice that the concentrations of interest belong to the linear range of the developed biosensor. For the case of lactate, a mean value of 10.9 mM is reported in literature in the case of murine embryonic stem cells [20]. Since the linear range of the lactate biosensor is within 0.5 and 2.5 mM, the dilution 1:10 of the DMEM is also suitable in this case. A potential of +550 mV is applied to the electrochemical cell also in this case. The current is recorded for 5 min, but mean value and standard deviation are calculated when the system reaches the steady-state (approximately the last 3 min for each measurement). Baseline, corresponding to a concentration of 0 mM of substrate, is subtracted from each measurement. No crosstalk is observed when glucose is measured with an electrode functionalized with LOD, and vice versa.

3.3. Metabolites in proliferation and differentiation states

With the aforementioned assumptions, we employed randomly distributed carbon nanotubes onto screen-printed electrodes to develop biosensors for glucose and lactate detection in cell culture medium. We chose an exclusively neuronal system *in vitro*, the

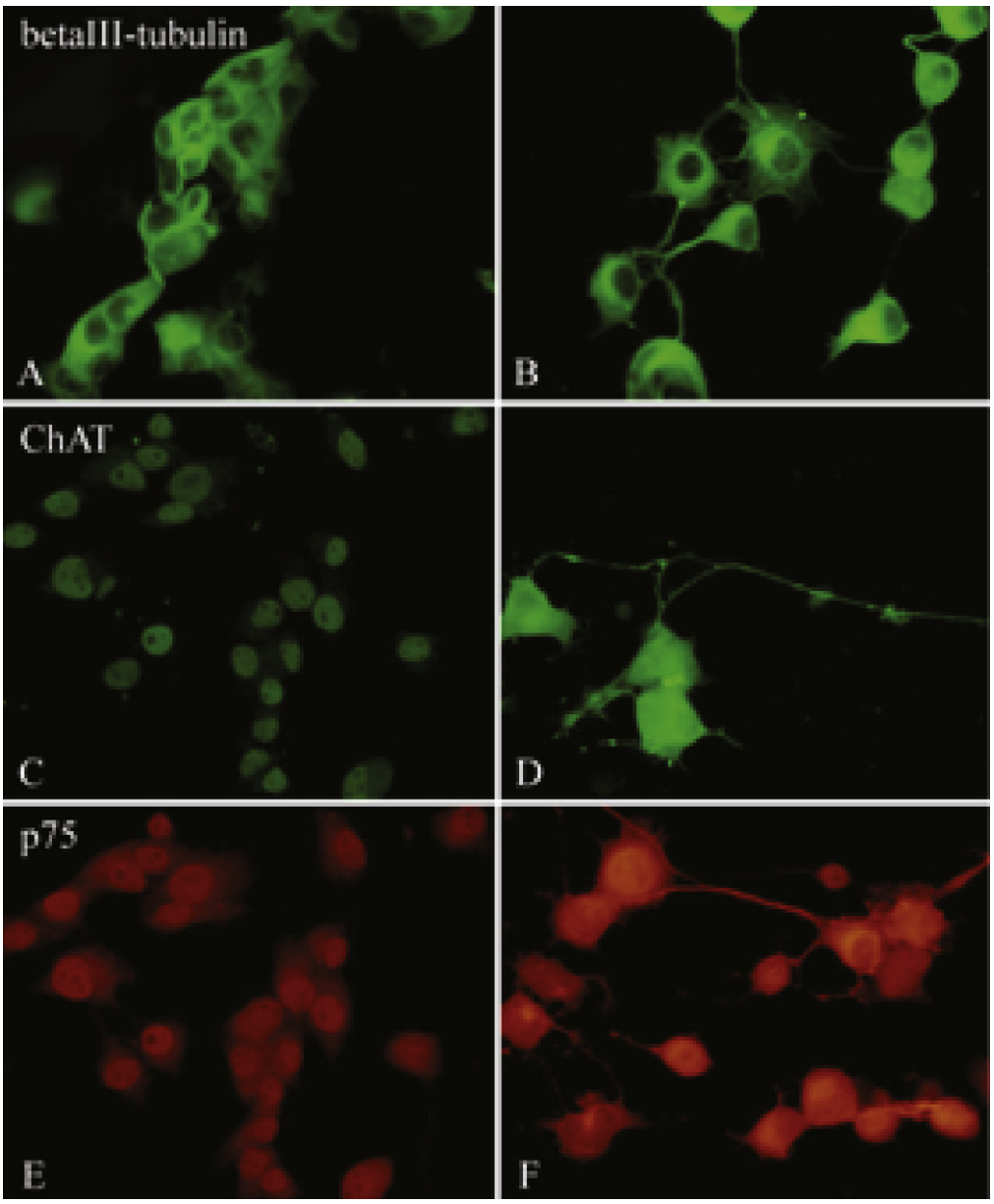

Fig. 3. Images from optical microscopy of different cell culture experiments. Neuronal phenotype is induced by 48 h exposure to RA, as indicated by morphology (βIII-tubulin before (A) and after (B) RA supply), neurochemical marker expression (ChAT–immunoreactivity before (C) and after (D) RA supply) and cholinergic marker expression (nerve growth factor low affinity receptor p75 before (E) and after (F) RA supply).

SN56 cell line. We validate and characterize our *in vitro* system by analyzing cell morphology, expression of neuronal and cholinergic markers, and cell viability both in proliferation and in differentiation phases.

Neuronal phenotype is induced by 48 h exposure to RA, as indicated by branched arborization (Fig. 3A and B, betaIII-Tubulin) and expression of neurochemical marker associated with mature cholinergic phenotype (Fig. 3C and D, ChAT-immunoreactivity; Fig. 3E and F, nerve growth factor low affinity receptor (p75)-immunoreactivity). To verify the effect of treatment with RA on cell number, cell viability is evaluated at a cell density of 2.5×10^4 cell cm^{-2} by MTT assay. SN56 proliferation is confirmed by the progressive increase of viable cells over the culture time (superimposed bars on Fig. 4A and C), whereas RA exposure results in a decrease of viability over the culture time, confirming the interruption of proliferation (bars on Fig. 4B and D) [15].

These neurons uptake glucose from the medium, and partly convert it via anaerobic glycolysis into lactate. Assuming this metabolic mechanism, we plate the SN56 cells at different cell concentrations, collecting surnatants at 3 time points, to challenge our sensor with different glucose consumption (Fig. 4A and B) and lactate production rates (Fig. 4C and D). Therefore, we compare metabolite dynamics during proliferation (Fig. 4A and C) and differentiation (Fig. 4B and D) conditions (obtained in the absence and in the presence of RA, respectively), to validate our sensors for neural cell monitoring.

Nanostructured sensors detect a progressive uptake of glucose in the media over the time, depending on cell density and time in culture, as illustrated in Fig. 4A and B. Glucose uptake in mature neurons (Fig. 4B) occurs at a lower rate than in proliferating cells (Fig. 4A), with the exception of the lowest cell density. It can be also observed that glucose concentration changes extremely fast in the case of proliferating cells

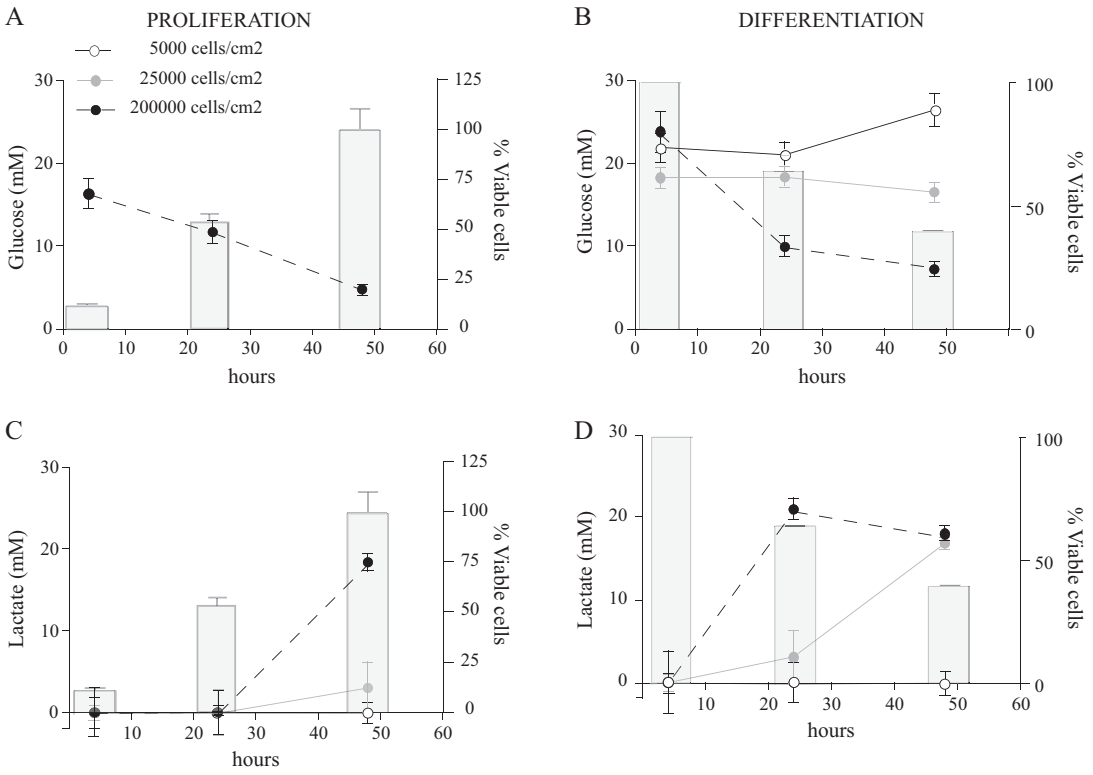

Fig. 4. Effect of cell density and state on glucose and lactate levels in cell cultures. Dot-plots represent glucose (A) and (B) and lactate (C) and (D) concentrations (indicated on left *y*-axis) in SN56 supernatants collected from cell cultures at three different densities, at 4, 24, 48 h (as indicated on the *x*-axis). The superimposed bar graphs point out the results of the cell viability assays in proliferation (A) and (C) and differentiation (B) and (D) media. The right *y*-axis indicates the percentages of viable cells respect to the control groups (100% of viable cells). Data are represented as means ± SD (dot-plots) or SEM (bar-graphs).

(Fig. 4A), while shows more stable curves during differentiation (Fig. 4B).

Neuronal lactate production in proliferating and differentiating cells is demonstrated by Fig. 4C and D, respectively. Lactate levels progressively rise accordingly to cell number and proliferation/differentiation state, in a symmetrical manner with respect to glucose shapes. A sharp decrease in glucose concentration, as obtained with higher cell densities, corresponds to an increase of the same extent in lactate levels. Furthermore, lactate production is affected by cell state, occurring earlier and in a sharper manner in differentiating cells (Fig. 4D) than during proliferation (Fig. 4C). Note that in the case of 5×10^3 cell cm^{-2}, lactate amount is below the detection limit of the sensor. Glucose and lactate behaviors found with the developed biosensors are also confirmed by measurements performed with a commercially available spectrophotometer assay (data not shown).

3.4. Measurements in glucose deprivation

To further explore the effectiveness of our biosensors in monitoring cell state changes, we dramatically modified neuronal metabolism by removing glucose from the culture medium, thereby inducing a metabolic stress. The glucose deprivation model is then applied to SN56 cultures after 48 hours of proliferation or differentiation, and both glucose (Fig. 5A and B) and lactate (Fig. 5C and D) were measured in the surnatants.

Fig. 5A and B describe glucose levels in complete and glucose-free culture medium in proliferating and differentiating cells, respectively. Glucose levels are low and stable at this time, independently of cell state (Fig. 5A and B, grey round dots), while values in deprived media are below the detection limit of the sensor (Fig. 5A and B, white square dots). Fig. 5C and D describe lactate levels in complete and glucose-free media, in proliferating and differentiating cells, respectively. Lactate levels are higher and more dynamic in the proliferating cultures (Fig. 5C and D, grey round dots) than in the differentiated ones (Fig. 5C and D, white square dots). The superimposed bars refer to cell viability measured by MTT assay in presence (grey bars) or absence (white bars) of glucose, and clearly indicate cell death in glucose-deprived cells, particularly in the case of differentiating cells.

Cell death induced by glucose deprivation was previously reported in SN56 cells [21,22] and neurons in culture [23]. SN56 is a line of cholinergic neurons which are highly sensitive to several stressors and to metabolic alterations. The interest about cholinergic neurons is connected to Alzheimer's disease, where their early loss is associated with a metabolic impairment in brain, whose extent is proportional to the severity of the cognitive deficits [24,25]. Furthermore, RA treatment increases SN56 vulnerability to oxidative stress, as demonstrated by an increase of caspase-3 mediated cell death [26,27] and lactate dehydrogenase activity, which is responsible for lactate production and consumption [28]. From the detected responses we can infer that the amount of glucose is not enough for a correct cell feeding, as recorded just after 4 h. Coherently, in proliferating cells our biosensors measure a massive lactate production after 4 hours, followed by a dramatic decrease within 24 h, and a sharp increase between 24 and 48 h. Furthermore, our results show that in actively proliferating cells, the lack of glucose for 24 h results in the consumption of neuronal lactate, dynamically released into the medium.

These data confirm the idea that glucose consumption during increased neuronal activity might be nonoxidative [29–31] and results in lactate production. It has been hypothesized that astrocytes may produce lactate during neuronal activation. Lactate is then oxidized by neurons to yield energy, playing a neuroprotective

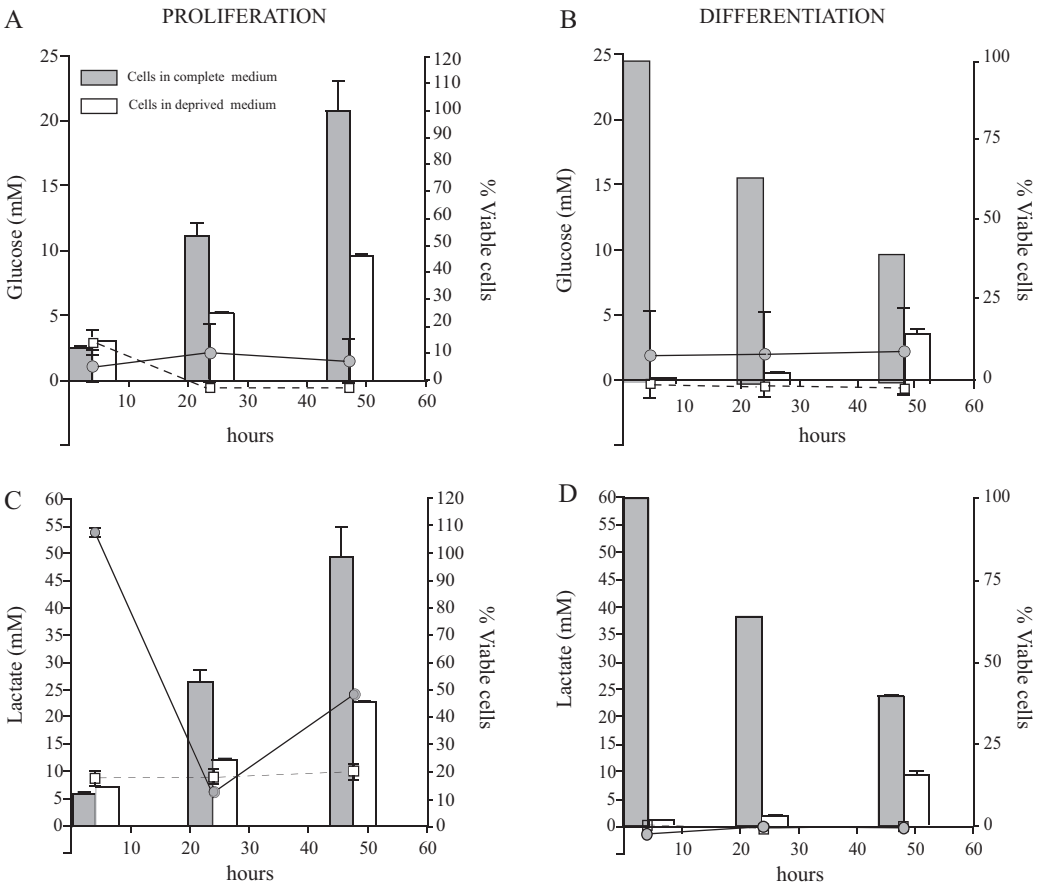

Fig. 5. Effect of glucose deprivation on glucose and lactate levels in cell cultures. Dot-plots represent glucose (A) and (B) and lactate (C) and (D) concentrations (indicated on left *y*-axis) in SN56 supernatants collected from cell cultures at the time-points indicated on the *x*-axis. The superimposed bar graphs point out the results of the cell viability assays in complete and deprived media, both in proliferation (A) and (C) and differentiation (B) and (D) conditions. The right *y*-axis indicates the percentages of viable cells respect to the control groups (100% of viable cells). Glucose and lactate concentration have been calculated using the standard curve. Data are represented as means ± SD (dot-plots) or SEM (bar-graphs).

role after cerebral ischemia [32,33]. According to other authors, oxidation of lactate by neurons would only be possible if the glycolytic consumption of glucose or its transport were inhibited [34]. The cellular system employed in this study contains uniquely neuronal cells [35]. Thus, it offers the chance to make assumptions about neuronal behavior.

4. Conclusion

The present research is focused on the development of nanostructured electrodes by using multi-walled carbon nanotubes for metabolite detection in cell culture medium. We show how nanostructuration can significantly improve the sensitivity of biosensors, while functionalization with oxidases offers high specificity. SEM images of the electrodes show that CNT form bundles and the protein layer wraps each carbon nanotube, forming a single layer of proteins onto nanotube surface. The measured thickness of CNT confirms this hypothesis. Then, we calibrate the developed biosensor for the detection of glucose and lactate. For glucose we found a sensitivity of 27.7 $\mu A\,mM^{-1}\,cm^{-2}$, a linear range within 0.5–4.0 mM, a detection limit of 73 μM. For lactate we observed a sensitivity of 40.1 $\mu A\,mM^{-1}\,cm^{-2}$, a linear range within 0.5–2.5 mM, and detection limit of 28 μM. We tested our biosensors in a cell culture along 48 h and we record the different behavior of such metabolites. Results clearly show a glucose uptake and a lactate production over the time, and different rate according to different cell seeding and cell state. Concentrations vary faster in proliferation state, while they are more stable during differentiation. Moreover, lactate dynamics progressively change in a symmetrical manner with respect to glucose shape, confirming the strong relationship between these two metabolites. Finally, we monitor lactate level in glucose deprivation conditions. The data confirm the idea that the oxidation of lactate is possible when the glycolytic consumption of glucose is inhibited, offering the chance to make assumption about neuronal behavior. Whereas it is still under debate the fate of neuronal or astrocytic lactate produced by glycolysis, our sensors provide new insight because of their higher sensitivity with respect to the state-of-the-art [36]. Indeed, our experiments have measured a production and uptake of lactate in neuronal cell cultures. The possibility to functionalize nanomaterials with different oxidases opens to the possibility of monitoring many different compounds, offering unique properties to enhance the detection of metabolites released in cell cultures.

Acknowledgements

The authors thank Marco Cantoni and Fabienne Bobard for acquisition of SEM images. S.C. and C.B. thank Giuseppe Dino Albini for deep discussions on sensitivity enhancement due to carbon nanotubes. Financial support from the Swiss Science National Foundation (grant n. IZLCZ2 123967 by Sino-Swiss cooperation) for the project “Nano-structured biochip development for stem cell monitoring” is greatly acknowledged.

Appendix A. Supplementary data

Supplementary data associated with this article can be found, in the online version, at doi:10.1016/j.snb.2011.03.053.

References

[1] D.A. Heller, H. Jin, B.M. Martinez, D. Patel, B.M. Miller, T.-K. Yeung, P.V. Jena, C. Hobartner, T. Ha, S.K. Silverman, M.S. Strano, Multimodal optical sensing and analyte specificity using single-walled carbon nanotubes, Nat. Nanotechnol. 4 (2009) 114–120.

[2] A. Poscia, M. Mascini, D. Moscone, M. Luzzana, G. Caramenti, P. Cremonesi, F. Valgimigli, C. Bongiovanni, M. Varalli, A microdialysis technique for continuous subcutaneous glucose monitoring in diabetic patients (part 1), Biosens. Bioelectron. 18 (2003) 891–898.

[3] A. Poscia, D. Messeri, D. Moscone, F. Ricci, F. Valgimigli, A novel continuous subcutaneous lactate monitoring system, Biosens. Bioelectron. 20 (2005) 2244–2250.

[4] J.J. Gooding, Nanostructuring electrodes with carbon nanotubes: a review on electrochemistry and applications for sensing, Electrochim. Acta 50 (2005) 3049–3060.

[5] L. Qiao, et al., First-principles density-functional investigation of the effect of water on the field emission of carbon nanotubes, Nanotechnology 18 (2007) 155707.

[6] A. Mayer, N.M. Miskovsky, P.H. Cutler, Theoretical comparison between field emission from single-wall and multi-wall carbon nanotubes, Phys. Rev. B 65 (2002) 155420.

[7] Y. Chen, D.T. Shaw, L. Guo, Field emission of different oriented carbon nanotubes, Appl. Phys. Lett. 76 (2000) 2469–2471.

[8] S. Carrara, V.V. Shumyantseva, A.I. Archakov, B. Samorì, Screen-printed electrodes based on carbon nanotubes and cytochrome P450scc for highly sensitive cholesterol biosensors, Biosens. Bioelectron. 24 (2008) 148–150.

[9] G. Dukovic, B.E. White, Z. Zhou, F. Wang, S. Jockusch, M.L. Steigerwald, T.F. Heinz, R.A. Friesner, N.J. Turro, L.E. Brus, Reversible surface oxidation and efficient luminescence quenching in semiconductor single-wall carbon nanotubes, J. Am. Chem. Soc. 126 (2004) 15269–15276.

[10] M. Grujicic, G. Cao, B. Gersten, Enhancement of field emission in carbon nanotubes through adsorption of polar molecules, Appl. Surf. Sci. 206 (2003) 167–177.

[11] L. Pellerin, P.J. Magistretti, Food for thought: challenging the dogmas, J. Cereb. Blood Flow Metab. 23 (2003) 1282–1286.

[12] L. Pellerin, P.J. Magistretti, Glutamate uptake into astrocytes stimulates aerobic glycolysis: a mechanism coupling neuronal activity to glucose utilization, Proc. Natl. Acad. Sci. U.S.A. 91 (1994) 10625–10629.

[13] R. Jolivet, I. Allaman, L. Pellerin, P.J. Magistretti, B. Weber, Comment on recent modeling studies of astrocyte-neuron metabolic interactions, J. Cereb. Blood Flow Metab. (2010) 1–5.

[14] H.J. Lee, D.N. Hammond, T.H. Large, B.H. Wainer, Immortalized young adult neurons from the septal region: generation and characterization, Dev. Brain Res. 52 (1990) 219–228.

[15] M.A. Malik, C.E. Greenwood, J.K. Blusztajn, B. Berse, Cholinergic differentiation triggered by blocking cell proliferation and treatment with all-trans-retinoic acid, Brain Res. 874 (2000) 178–185.

[16] S.O. Nielsen, G. Srinivas, C.F. Lopez, M.L. Klein, Modeling surfactant adsorption on hydrophobic surfaces, Phys. Rev. Lett. 94 (2005) 228301.

[17] G. Wohlfahrt, S. Witt, J. Hendle, D. Schomburg, H.M. Kalisz, H. -J, Hecht 1. 8 and 1. 9 A resolution structures of the Penicillium amagasakiense and Aspergillus niger glucose oxidases as a basis for modelling substrate complexes, Acta Crystallogr. D 55 (1999) 969–977.

[18] S.J. Li, Y. Umena, K. Yorita, T. Matsuoka, A. Kita, K. Fukui, Y. Morimoto, Crystallographic study on the interaction of L-lactate oxidase with pyruvate at 1.9 A resolution, Biochem. Biophys. Res. Commun. 358 (2007) 1002–1007.

[19] C. Boero, S. Carrara, G. De Micheli, Sensitivity enhancement by carbon nanotubes: applications to stem cell cultures monitoring, in: Research in Microelectronics and Electronics, 2009, PRIME 2009. Ph. D., 2009, pp. 72–75.

[20] Y.-S. Hwang, J. Cho, F. Tay, J.Y.Y. Heng, R. Ho, S.G. Kazarian, D.R. Williams, A.R. Boccaccini, J.M. Polak, A. Mantalaris, The use of murine embryonic stem cells, alginate encapsulation, and rotary microgravity bioreactor in bone tissue engineering, Biomaterials 30 (2009) 499–507.

[21] L.V Colom, M.E. Diaz, D.R. Beers, A. Neely, W.J. Xie, S.H. Appel, Role of potassium channels in amyloid-induced cell death, J. Neurochem. 70 (1998) 1925–1934.

[22] A.C.N. Pinheiro, R.S. Gomez, A.R. Massensini, M.N. Cordeiro, M. Richardson, M.A. Romano-Silva, M.A.M. Prado, L.D. Marco, M.V. Gomez, Neuroprotective effect on brain injury by neurotoxins from the spider Phoneutria nigriventer, Neurochem. Int. 49 (2006) 543–547.

[23] B. Páramo, K. Hernández-Fonseca, A.M. Estrada-Sánchez, N. Jiménez, A. Hernández-Cruz, L. Massieu, Pathways involved in the generation of reactive oxygen and nitrogen species during glucose deprivation and its role on the death of cultured hippocampal neurons, Neuroscience 167 (2010) 1057–1069.

[24] G.E. Gibson, L.C.H. Park, K.-F.R. Sheu, J.P. Blass, N.Y. Calingasan, The [alpha]-ketoglutarate dehydrogenase complex in neurodegeneration, Neurochem. Int. 36 (1999) 97–112.

[25] T. Sawamura, K. Shimizu, M. Nibuya, T. Wakizono, G. Suzuki, T. Tsunoda, Y. Takahashi, S. Nomura, Effect of paroxetine on a model of post-traumatic stress disorder in rats, Neurosci. Lett. 357 (2004) 37–40.

[26] U. Fass, K. Panickar, D. Personett, D. Bryan, K. Williams, J. Gonzales, K. Sugaya, M. McKinney, Differential vulnerability of primary cultured cholinergic neurons to nitric oxide excess, Neuroreport 11 (2000) 931–936.

[27] D. Personett, U. Fass, K. Panickar, M. McKinney, Retinoic acid-mediated enhancement of the cholinergic/neuronal nitric oxide synthase phenotype of the medial septal sn56 clone, J. Neurochem. 74 (2000) 2412–2424.

[28] A. Szutowicz, A. Jankowska, J.K. Blusztajn, M. Tomaszewicz, Acetylcholine and acetyl-CoA metabolism in differentiating SN56 septal cell line, J. Neurosci. Res. 57 (1999) 131–136.

[29] T.G. Bolwig, B. Quistorff, *In vivo* concentration of lactate in the brain of conscious rats before and during seizures: a new ultra-rapid technique for the freeze-sampling of brain tissue, J. Neurochem. 21 (1973) 1345–1348.

[30] P.T. Fox, M.E. Raichle, Focal physiological uncoupling of cerebral blood flow and oxidative metabolism during somatosensory stimulation in human subjects, Proc. Natl. Acad. Sci. U.S.A. 83 (1986) 1140–1144.

[31] P.T. Fox, M.E. Raichle, M.A. Mintun, C. Dence, Nonoxidative glucose consumption during focal physiologic neural activity, Science 241 (1988) 462–464.

[32] A.-K. Bouzier-Sore, P. Voisin, P. Canioni, P.J. Magistretti, L. Pellerin, Lactate is a preferential oxidative energy substrate over glucose for neurons in culture, J. Cereb. Blood Flow Metab. 23 (2003) 1298–1306.

[33] C. Berthet, H. Lei, J. Thevenet, R. Gruetter, P.J. Magistretti, L. Hirt, Neuroprotective role of lactate after cerebral ischemia, J. Cereb. Blood Flow Metab. 29 (2009) 1780–1789.

[34] M.A. Castro, F.A. Beltrán, S. Brauchi, I.I. Concha, A metabolic switch in brain: glucose and lactate metabolism modulation by ascorbic acid, J. Neurochem. 110 (2009) 423–440.

[35] D.N. Hammond, H.J. Lee, J.H. Tonsgard, B.H. Wainer, Development and characterization of clonal cell lines derived from septal cholinergic neurons, Brain Res. 512 (1990) 190–200.

[36] S. Carrara, C. Boero, G. Micheli, Quantum dots and wires to improve enzymes-based electrochemical bio-sensing, in: A. Schmid, S. Goel, W. Wang, V. Beiu, S. Carrara (Eds.), Nano-Net, Springer, Berlin Heidelberg, 2009, pp. 189–199.

Biographies

Cristina Boero received her MS degree in biomedical engineering from Politecnico di Torino, Italy, in 2007. During the Master thesis, she joined the École Polytechnique Fédérale de Lausanne (EPFL), Switzerland. She has been a doctoral candidate at Laboratory of Integrated Systems since 2009. Her main interest is on electrochemical biosensors for the detection of metabolites in stem cell cultures. The goal is to develop a fully integrate chip to detect such metabolites in real-time into Petri dishes. She is also interested in the functionalization of electrodes with nanostructures, like carbon nanotubes, and the interaction between proteins and nanostructures.

Sandro Carrara is a Senior Scientist at the EPFL and Professor of nano-bio-sensing and micro/nano interfaces at the Department of Electrical Engineering and Biophysics (DIBE) of the University of Genoa. His scientific interests are on electrical phenomena of nano-bio-structured films, with special focus on Protein and DNA biochips. He has more than 90 scientific publications and 10 patents. His work was awarded in several International Symposiums. He is Founder and Editor-in-Chief of BioNanoScience journal, and Associate Editor of two IEEE Transactions. He is in several Boards of International Conferences on Circuits and Systems for Biomedical Applications.

Giovanna Del Vecchio received her degree in Medical Biotechnologies from the University of Bologna (Italy) in 2004 and a Ph.D. degree in Biotechnological tools for Neuro-morpho-physiology at the same university in 2009. Her research activity is mainly focused on CNS diseases through *in vitro* and *in vivo* models of neurodegeneration. The main aim of her investigations was to identify the crucial network of molecules involved in CNS diseases that can restore the endogenous self repair response in the damaged tissue. From 2009 to 2010, she worked as a post-doctoral fellow at the University of Bologna and as visiting scientist at the EPFL (Switzerland). She is currently working as a post-doctoral fellow at the FMP-Leibniz Institute (Germany) on the modulation of the blood brain barrier to improve the drug delivery in the CNS. Dr Del Vecchio has co-authored eight refereed journal papers and 19 conference papers and abstracts.

Laura Calzà, MD, professor of Veterinary Anatomy, Director of the Interdipartimental Centre for Industrial Research Health Science and Technology (ICIR-HST) at University of Bologna, Italy. Neurobiologist, she is an expert *in vitro* and *in vivo* modeling for neurodegenerative diseases and dynamic imaging. Main focus of her research activity is the study of reactive and repair mechanisms of the nervous system following experimental and spontaneous lesions, according to the bench-to-bedside approach of the translational medicine. Regenerative medicine for CNS using cell/scaffolds combined devices represents the most advanced area of interest. The lab belongs to the high-technology Laboratory network of Emilia Romagna region. She is author of more than 140 papers on referred journals.

Giovanni De Micheli is Professor and Director of the Institute of Electrical Engineering and of the Integrated Systems Centre at EPFL, Switzerland. He is program leader

of the Nano-Tera.ch program. Prof. De Micheli is a Fellow of ACM and IEEE and a member of the Academia Europaea. His research interests include several aspects of design technologies for integrated circuits and systems, such as synthesis for emerging technologies, networks on chips and 3D integration. He is also interested in heterogeneous platform design including electrical components and biosensors, as well as in data processing of biomedical information. Prof. De Micheli is the recipient of the 2003 IEEE Emanuel Piore Award for contributions to computer-aided synthesis of digital systems. He received the Golden Jubilee Medal for outstanding contributions to the IEEE CAS Society in 2000. He received the 1987 D. Pederson Award for the best paper on the IEEE Transactions on CAD/ICAS, two Best Paper Awards at the Design Automation Conference, in 1983 and in 1993, and a Best Paper Award at the DATE Conference in 2005.